Condensation by heterogeneous nucleation in a thermal boundary layer

M. S. Chen
Industrial and Engineering Technology, Central Michigan University, Mt. Pleasant, MI, USA

B. W. Jones
Institute for Environmental Research, Kansas State University, Manhattan, KS, USA

Condensation can occur by the nucleation and growth of water droplets on particles in the air. This mode of mass transport can readily occur in a thermal boundary layer. The primary condition required for droplet nucleation is the existence of supersaturation in the boundary layer. Equations are developed to describe droplet nucleation and transport for the boundary layer on a horizontal, upward facing surface. These equations allow diffusion and nucleation mass fluxes and droplet concentration at a point in the boundary layer to be calculated. Experimental data were collected and compared to the theoretical calculations. Accurately predicting droplet concentration is difficult, but the presence of nucleation condensation can be readily predicted.

Keywords: condensation; heterogeneous nucleation; boundary layer

Introduction

Most moisture condensation phenomena can be described as a process of water vapor diffusion through air with condensation on a chilled surface. Figure 1(a) shows velocity, temperature, and water vapor density profiles for a typical boundary-layer problem of this nature. The vapor density and the temperature vary continuously throughout the boundary layer. Under some conditions the temperature and vapor density can be such that the air becomes supersaturated within the boundary layer. Such conditions generally occur when the temperature difference between the air stream and the chilled surface is very large and/or when the air stream is very nearly saturated. Figure 1(b) shows a saturation profile for this situation. Supersaturated air in the boundary layer gives rise to the possibility of a second mechanism for condensation: nucleation of droplets in the boundary layer. There are two forms of such nucleation: (1) heterogeneous nucleation and (2) homogeneous nucleation. Heterogeneous nucleation refers to the nucleation of droplets on other particles in the air. Homogeneous nucleation refers to the nucleation of droplets with no foreign matter serving as a nucleation site and is sometimes referred to as spontaneous nucleation. Homogeneous nucleation generally requires saturations much greater than unity, which occur only in extreme situations. We do not discuss it further in this article. Heterogeneous nucleation can occur with supersaturations only slightly greater than unity. All but the most highly filtered air has sufficient foreign material to provide a large number of nucleation locations, because even submicron-sized particles can serve as nucleation sites. Heterogeneous nucleation has been studied extensively in connection with cloud physics,[1–3] but no research on heterogeneous nucleation in boundary-layer situations has been reported.

Address reprint requests to Dr. Chen at Industrial and Engineering Technology, Central Michigan University, Mt. Pleasant, MI 48859, USA.

Received 1 December 1989; accepted 5 July 1990

Figure 2 gives an overview of the process of heterogeneous nucleation in a horizontal laminar boundary layer. The process along only one streamline is shown for clarity, but similar processes occur along other streamlines that enter the supersaturation zone. Air containing particles enters the boundary

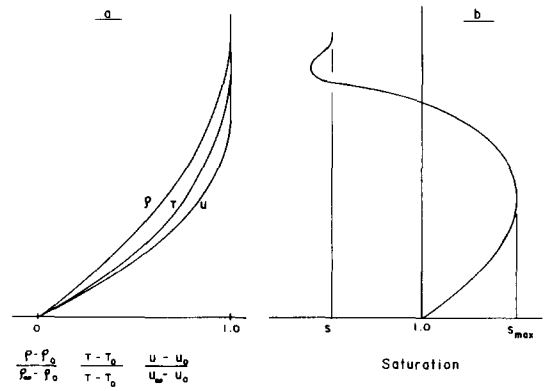

Figure 1 Boundary-layer profiles

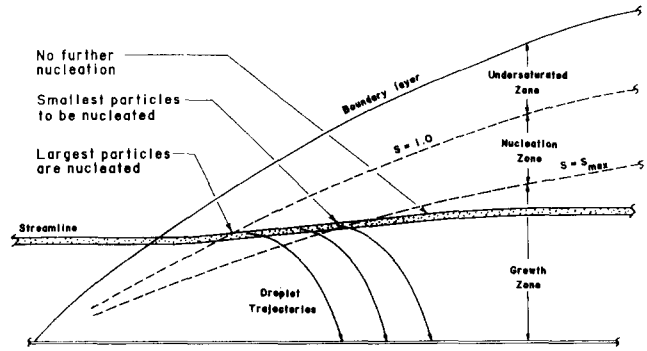

Figure 2 Heterogeneous nucleation in a boundary layer

layer as shown. As the boundary layer grows, the streamline moves farther into the boundary layer and eventually encounters the supersaturated air. The supersaturation boundary is similar in shape to the boundary layer. The particles that make the best nucleation sites are nucleated first. As the air passes farther into the supersaturation zone and into more highly saturated air, additional particles nucleate. Eventually, the air reaches a point where supersaturation is insufficient to nucleate additional droplets. This condition generally occurs where the supersaturation starts to decrease. The droplets that are nucleated continue to grow so long as they remain in the supersaturated air. The unnucleated particles follow the streamlines quite well, at least at low air velocities. However, the droplets generally become large enough that they no longer follow the streamline. In the situation shown in Figure 2, they fall to the chilled horizontal surface.

The purposes of this study were to develop mathematical equations to describe this process of heterogeneous nucleation in boundary layers, to combine these equations with appropriate boundary-layer equations to develop a model that could predict the amount of condensation by heterogeneous nucleation and the number and size of droplets formed, and experimentally to measure heterogeneous nucleation to provide data with which to evaluate the model's accuracy.

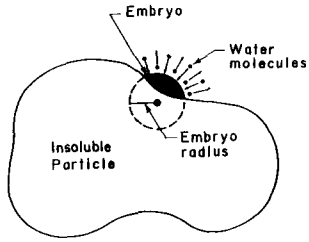

Figure 3 Nucleation on an insoluble particle

Theoretical analysis

The presence of heterogeneous nucleation in the boundary layer complicates the description of the heat and mass transfer processes. The vapor pressure profile is altered by removal of vapor from the air by droplet nucleation and growth. Similarly, the temperature profile is altered by the latent heat of vaporization associated with condensation on the droplets or evaporation of the droplets. Thus the nucleation equations must be solved simultaneously with the energy and mass equations for the boundary layer. Nucleation has only a secondary effect on the velocity profile in the boundary layer, so the hydrodynamic equations can be solved independently.

In order to reduce complexity—and to focus on the nucleation condensation phenomena—a one-dimensional (1-D) analysis of simultaneous heat and mass transfer was used in this study.[4,5] The thickness of the hydrodynamic boundary layer was determined without considering the effects of nucleation. The thermal and diffusional boundary-layer thicknesses were then found using the Prandtl and Schmidt numbers. These thicknesses were then assumed not to change as a result of nucleation in the boundary layer. The mass and energy equations then are[6]

$$\frac{d\rho_v}{dy}=\frac{1}{D}\left(\frac{\rho_v}{\rho}-1\right)(\dot{M}-n_c) \tag{1}$$

and

$$\frac{dT}{dy}=\frac{1}{K}(\dot{M}c_pT-n_cL-\dot{Q}) \tag{2}$$

where $\dot{M}$ is the total mass flux through the boundary layer and

Notation

$C(r)$	Concentration variation of atmospheric particles with size
$\overline{C_d}$	Local droplet concentration
C_o	Dust particle concentration constant
c_p	Specific heat of vapor
D	Diffusion coefficient of water–air
g	Gravitational acceleration
i	Ionic potential of solute (typically about 2.0)
J	Nucleation rate of dust particles
K	Thermal conductivity of air
L	Latent heat of vaporization for water
m	Mass of a droplet
m_s	Mass of solute
m_w	Mass of water
M_v	Molecular weight of water
M_s	Molecular weight of solute
$\dot{M}$	Overall mass flux crossing the boundary layer
n_c	Local mass flux of condensation
n_d	Droplet flux
N_p	Pulse number of signal collection
P	Local vapor pressure
P_s	Equilibrium vapor pressure
$\dot{Q}$	Overall heat flux crossing the boundary layer
r	Local droplet radius
r_c	Critical particle radius
r_0	Initial droplet radius
r_s	Equilibrium radius of a solution particle
r^*	Critical droplet or embryo radius
R	Particle radius
$\bar{R}$	Universal gas constant
S	Saturation, P/P_s
t	Time
T	Local temperature
u	Local horizontal velocity component inside the hydrodynamic boundary layer
v	Droplet velocity, vertical
V	Scattering volume
y	Vertical coordinate with the origin at the edge of the diffusional boundary layer
y'	Location at which a droplet nucleated

Greek symbols

θ	Angle between sublayer and streamline
α	Contact angle between embryo and particle surface
ϕ	Moisture available for nucleation (dimensionless)
δ_n	Width of nucleation zone
δ_D	Diffusional boundary layer thickness
π	Transient time of droplets
ρ	Total density of air and vapor
ρ_L	Density of liquid water
ρ_v	Density of vapor
τ_s	Scan time for signal recording
μ	Dynamic viscosity of air
σ	Surface tension of water on a flat liquid surface

$\dot{Q}$ is the total heat flux through the boundary layer, both of which are constant with distance through the boundary layer (y). Note that y is defined as distance from the edge of the diffusional boundary layer rather than distance from the surface. The mass transported in condensed form is n_c and the term

$$\dot{M}c_pT - n_cL$$

represents the heat flux alteration caused by latent heat of vaporization of the condensed liquid. This term neglects any temperature difference between the droplets and the surrounding air.

The condensed mass flux, $n_c(y)$, can be calculated by addressing nucleation rates and subsequent droplet growth. The radius of a droplet at y is

$$r = r_0 + \int_{y'}^{y} \left\{\frac{dr}{dy}\right\} dy \tag{3}$$

where y' is the location where the nucleation occurs and r_0 is the initial radius of a nucleated droplet. The mass of a droplet then is

$$m = \rho_L \frac{4\pi}{3}\left[r_0 + \int_{y'}^{y} \left\{\frac{dr}{dy}\right\} dy\right]^3 \tag{4}$$

The mass flux of particles at y from nucleation at y' is

$$dn_c(y) = mJ(y')\,dy' \tag{5}$$

where $J(y')$ is the droplet generation in terms of droplets per unit time per unit volume. However, droplets at y may have been nucleated at any location between the boundary-layer edge ($y=0$) and y. Equation 6 must then be integrated over this range to get the total condensed mass flux:

$$n_c(y) = \rho_L \frac{4\pi}{3}\int_0^y \left[r_0 + \int_{y'}^{y} \left\{\frac{dr}{dy}\right\} dy\right]^3 J(y')\,dy' \tag{6}$$

The generation rate of droplets, $J(y')$ and the droplet growth rate, dr/dy, must be described before Equation 6 can be evaluated. We address droplet generation first. The nucleation process has been described by a number of researchers.[1,2,7] In order for a water droplet to be nucleated, it must reach some critical size. Whether a droplet grows depends on the supersaturation present and the size of the droplet. If the droplet is too small, the increased vapor pressure from surface tension more than offsets the excess vapor pressure in the air from supersaturation, and the droplet will dissipate. If the droplet is sufficiently large, surface tension effects are insufficient to offset the excess vapor pressure and the droplet grows. The critical radius, r^*, of a water droplet—where the surface tension effect just offsets the excess vapor pressure—is

$$r^* = \frac{2M_v\sigma}{\rho_L \bar{R}T\ln(S)} \tag{7}$$

Any droplet with a radius larger than this critical value grows very rapidly and is said to be "nucleated."

The actual nucleation process depends on the nature of the foreign material present, especially on whether the material is soluble or insoluble. Figure 3 shows the process on an insoluble particle. Water embryos form on the particle because of the random motion of the molecules. The embryos normally dissipate rapidly, as they are smaller than the critical size in Equation 7. If an embryo forms with a radius larger than the critical radius of a water droplet, it continues to grow, and a water droplet is nucleated. This nucleation process is stochastic in nature, and we cannot say with certainty which particles serve as nucleation sites for given environmental conditions. The rate of embryo formation is extremely sensitive to supersaturation, however, and an increase in supersaturation of a small fraction of 1 percent can increase the probability of nucleation from essentially zero to essentially unity. Thus critical conditions can be defined for which a given particle can be assumed to nucleate. Fletcher[8] derived a relationship that describes the dependence of the nucleation rate on supersaturation. This relationship can be used to determine the critical conditions.[6] In addition to supersaturation, Fletcher shows that the nucleation rate for insoluble particles depends on the contact angle between the embryo and the particle surface, α, and also on particle size. Using Fletcher's relationship, a critical particle radius, r_c, can be defined for any supersaturation. Any particle larger than this size is nucleated, and any particle smaller is not. This critical radius depends on supersaturation and particle surface characteristics, which are described by α.

Droplet nucleation on soluble material results from a different process. Moisture from the air diffuses to the soluble material and forms a solution. The resulting "particle," which normally is a liquid, gains or loses moisture until the concentration of the solute reaches equilibrium. At equilibrium, the depression in vapor because of the solute and the increase in vapor pressure because of surface tension offset each other, so that the particle is in equilibrium with the ambient vapor pressure. This equilibrium radius, r_s, can be calculated using the reasoning of Rogers and Yau:[9]

$$r_s = \frac{2M_v\sigma}{\rho \bar{R}T\ln(S/a)} \tag{8}$$

where

$$a = 1 - i\frac{m_s M_v}{m_w M_s}$$

Thus solution particles are different from the embryos on insoluble particles. The embryos are unstable and either grow or dissipate. The solution particles are stable and neither grow nor dissipate if the saturation does not change. There is, however, a critical supersaturation for a given amount of solute. With this level of supersaturation there is no equilibrium and the particle continues to grow and is nucleated.

Table 1 shows the effect of supersaturation on nucleation for both soluble and insoluble particles. In the case of insoluble particles, there is a minimum supersaturation below which no particle nucleates, regardless of its size. Above this supersaturation level, larger particles nucleate more readily than smaller particles. The situation is similar for solution particles. Below some minimum supersaturation level the particles grow (or shrink) to be in equilibrium with the ambient air; above this level they nucleate.

The conditions in this study yield maximum supersaturations of not more than 3 percent in most cases. Table 1 shows that insoluble particles do not nucleate with these conditions unless the contact angle is near zero. Insoluble particles that are active in nucleation then behave similarly to water droplets and Equation 7 should give a good approximation of their critical radii. A similar situation exists for solution particles. Table 1 shows that the radius at which these particles nucleate does not differ greatly from the critical radius for a water droplet. The droplet growth from saturated conditions ($S=1$) to the critical supersaturation is relatively small. Equation 7 also gives a fair approximation of the critical radius of solution particles, generally within a factor of 2. Consequently, we used Equation 7 for all nucleation calculations; we made no distinction between soluble and insoluble materials and ignored any nonwetted insoluble particles. This latter omission may not be too crucial. Mason[2] found evidence that insoluble particles

Table 1 Effect of saturation on particle nucleation†
(a) Soluble material (NaCl)

Solute (g)	10^{-16}	10^{-17}	10^{-18}	10^{-19}	0‡
Saturation	Particle radius at equilibrium (μm)				
1.001	0.050	0.023	0.0106	0.0049	1.033
1.002	0.051	0.023	0.0106	0.0049	0.516
1.005	0.054	0.024	0.0107	0.0049	0.207
1.010	0.077	0.025	0.0110	0.0050	0.103
1.020		0.031	0.0115	0.0051	0.052
1.030			0.0122	0.0052	0.035
1.050	———	Nucleated	———	0.0054	0.021
1.10				0.0068	0.0108
1.20					0.0057
s^*	1.010	1.022	1.047	1.105	—
r^* (μm)	0.078	0.036	0.168	0.0078	—

(b) Insoluble material

$\cos\alpha$	1.00	0.95	0.90
Saturation	Particle size required for nucleation (μm)		
1.01	0.103		
1.02	0.052	——No nucleation——	
1.05	0.021		
1.10	0.0108	0.0330	
1.20	0.0057	0.0095	0.034
1.50	0.0026	0.0035	0.0039

† All calculations for 300 K.
‡ Critical radii for pure water.

have a hygroscopic surface layer that allows them to be readily wetted.

The droplet generation rate now becomes:[6]

$$J(y')=u\tan\theta c(r)\frac{dr_c}{dy'} \tag{9}$$

where u is the local air velocity, θ is the angle between the streamline and the lines of constant temperature and vapor pressure in the boundary layer, and $C(r)$ is the particle concentration function. The derivative term in Equation 10 can be evaluated by

$$\frac{dr_c}{dy'}=\frac{\partial r_c}{\partial T}\frac{\partial T}{\partial y'}+\frac{\partial r_c}{\partial \rho_v}\frac{\partial \rho_v}{\partial y'} \tag{10}$$

In principle, the terms $\partial r_c/\partial T$ and $\partial r_c/\partial \rho_v$ can be evaluated from Equation 7. We did not attempt to solve for these derivatives, because the numerical techniques employed make this calculation unnecessary.

The particle concentration function in Equation 9 is still required in order for us to determine the droplet nucleation rate. Ideally, this distribution would be measured for a specific air source, but such measurements are generally not feasible. However, the theory of a self-preserving size distribution gives a good description for a wide range of situations.[10] It can be expressed as

$$C(r)=3C_o\left[\frac{1}{r_1^4}-\frac{1}{r_2^4}\right] \tag{11}$$

where r is the particle radius and C_o is a constant for a given air source. This constant indicates overall particle concentration and varies greatly from location to location.

The growth term, dr/dy, in Equation 6 must also be evaluated. The equation for droplet growth developed by Byers[1] is

$$r\frac{dr}{dt}=\frac{S-1}{\rho_L M_v L^2/K\bar{R}T^2+\rho_L\bar{R}T/M_v DP_s} \tag{12}$$

Equation 12 needs to be expressed in distance rather than in time to be compatible with Equation 6. For a horizontal boundary layer, the droplet can be assumed to fall at its terminal velocity, V, as described by Allen:[11]

$$v=\frac{2}{9}\frac{\rho_L g}{\mu}r^2 \tag{13}$$

The left-hand side of Equation 12 can be rearranged and combined with Equation 13 to give

$$r\frac{dr}{dt}=r\frac{dr}{dy}\frac{dy}{dt}=r\frac{dr}{dy}v=\frac{2}{9}\frac{\rho_L g}{\mu}r^3\frac{dr}{dy} \tag{14}$$

Equation 14 can now be used to express growth in terms of distance and—when combined with Equation 12—results in:

$$\frac{dr}{dy}=\left[\frac{9\mu}{2\rho_L g r^3}\right]\left[\frac{S-1}{\rho_L M_v L^2/K\bar{R}T^2+\rho_L\bar{R}T/M_v DP_s}\right] \tag{15}$$

A comment about the 1-D approach is in order at this point. The preceding equations treat the droplet as if it were falling vertically, whereas in reality it is also traveling horizontally while it falls, as shown in Figure 2. No major error is introduced if there is little change in the boundary-layer thickness from the point where the droplet nucleates to the point where it hits the surface. Thus the 1-D approach is limited to low-velocity air flows, where the droplets fall before traveling great distances. Other situations require a 2-D simulation of the boundary layer.

This set of equations along with information about various properties (e.g., saturation pressure, surface tension, diffusivity, etc.) provide the necessary expressions for describing the heterogeneous nucleation phenomenon and heat and moisture transport in the boundary layer.

We also want to know the droplet number density at a given point in the boundary layer. The total droplet flux at some point y is

$$n_d(y)=\int_0^y J(y')\,dy' \tag{16}$$

Droplet concentration at this same point depends not only on the flux but also on how fast the droplets are falling. However, the droplets have a range of radii, with droplets of each radius falling at a different velocity. The total droplet concentration at y then is

$$C_d(y)=\int_0^y \frac{J(y')}{v(y,y')}\,dy' \tag{17}$$

where $v(y, y')$ is the terminal velocity, according to Equation 13, of a droplet at y that was nucleated at y'. This velocity depends on the droplet radius at y, which can be evaluated by Equation 3.

A trial-and-error solution of the equations was required. We started the solution at the boundary-layer edge ($y=0$) and integrated the equations to the surface. Values of $\dot{M}$ and $\dot{Q}$ were required for this integration. Initial guesses were made by calculating heat and mass transfer with no nucleation. The values of vapor density and temperature at the surface obtained by integrating the equations were compared to the specified surface conditions. The values of $\dot{M}$ and $\dot{Q}$ were adjusted if necessary and the integration repeated. This process was repeated until the calculated conditions matched the surface conditions.

The solution was divided into three regions: (1) the under-

saturated zone, (2) the nucleation zone, and (3) the growth zone. In the undersaturated zone, no nucleation takes place and n_c is zero. Only Equations 1 and 2 need to be integrated, which we did by using a fourth-order Runge–Kutta method.

Once the integration enters the saturated zone, the nucleation phenomena must be addressed. To facilitate these calculations, we approximated the particle size distribution in Equation 11 with a discrete distribution. The particle radii were divided into 50 values, typically ranging from 0.03 μm to 3 μm. The radii were spaced logarithmically over this range. The smallest radius was sufficiently small that no smaller particles would be nucleated with the environmental conditions encountered. The largest radius represents radii with sufficiently low concentration that they become insignificant in number for the overall calculations. As the calculations entered the saturated zone, we checked the largest radius of particle to see whether it would nucleate at the local environmental condition, using Equation 7. If so, we assumed that all particles of that size nucleate. Then we checked the next smaller radius, and so on until reaching a radius that was sufficiently small that it would not nucleate. At the next step inward, this radius was the first one checked for nucleation as all larger radii were nucleated at previous locations. These calculations allow Equation 9 to be solved with the values of u and θ determined from the no-nucleation case. Once nucleated, the growth of the droplets was calculated with Equations 3 and 15 with r_o set to the radius of the nucleated particles. As the radii of droplets nucleated at different locations would be different at a given value of y, it was necessary to keep track of where each size of particle was nucleated and its subsequent growth. The total condensed mass flux, n_c, at a location, y, was then the sum of all nucleation and growth above that location, as described by Equation 6. This same information allowed Equation 17 to be readily solved to determine the droplet number density.

At some point in the solution, supersaturation began to decrease and no further nucleation took place. This region is referred to as the growth zone, as the droplets would normally continue to grow even though additional droplets would not form. Droplet growth and condensed mass flux calculations were the same as in the nucleation zone. All calculations regarding nucleation and droplet growth utilized first order Runge–Kutta integration, both in the growth zone and the nucleation zone. Also we assumed that the droplets did not coalesce.

Experimental measurements

In order to test the validity of the theoretical model, we devised a series of experiments to measure nucleation in a thermal boundary layer. Theoretical calculations indicated that the overall mass flux from droplet formation was not greatly affected by nucleation, at least for moderate environmental conditions. Typically, nucleation increased the mass flux by no more than 10 percent—and generally less. This small change in mass flux and the difficulty of separating the nucleation mass flux from the diffusion mass flux in experimental measurements indicated that some other measure of nucleation should be used. The experimental measurements thus focused on number density, because any droplets that appeared could be attributed to nucleation.

Figure 4 shows the experimental apparatus. A chilled flat plate was placed horizontally in the test section of a closed air-flow loop. The air-flow loop supplied air with a controlled temperature and humidity. The free-stream air velocity was measured with a hot film anemometer. A velocity of 0.15 m/s was used for all data collected. The humidity of the incoming air was measured with a chilled mirror dew-point hygrometer.

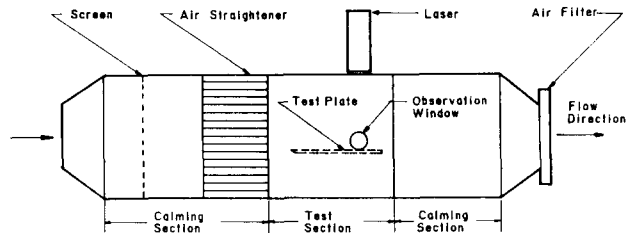

Figure 4 Experimental test section

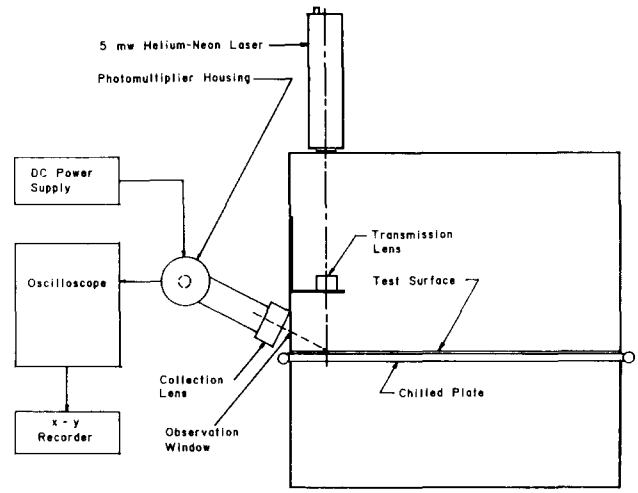

Figure 5 Optical counting system

The air temperatures and the temperature of the chilled plate were measured with thermocouples. A film of water completely covered the chilled plate and thermocouples during the experiments.

An optical counting system was used to measure the droplet number density. The basic system components are shown in Figure 5. A laser beam was vertically directed through the boundary layer. The beam was focused to a diameter of 0.55 mm immediately above the plate. A small window in the side of the test section allowed light scattered by the droplets to be detected by a photomultiplier tube. The scattered light was focused on the tube in such a way that it detected droplets between 1.6 mm and 5.6 mm above the plate. Thus a well-defined cylindrical measuring volume resulted. The measurements were made 610 mm from the leading edge, and the sample volume was well within the boundary layer. The output of the photomultiplier tube was connected to a digital storage oscilloscope. As the droplet passed through the measuring volume a "blip" appeared on the oscilloscope trace. A laser beam is not of uniform intensity but rather varies with a Gaussian distribution about the center of the beam. The resulting signal on the oscilloscope thus corresponded to this distribution of intensity. Figure 6 shows a typical oscilloscope trace. Each time a droplet passed through the measuring volume, a separate signal resulted. Different droplets have different amplitudes owing to differences in size. Also, some droplets pass through the edge of the beam where the intensity is low, and some pass through the center of the beam where the intensity is highest. This distribution, too, affects the intensity of the scattered light. The measuring system could not therefore be used to measure size distribution, because size effects could not be distinguished from path effects. Although the Gaussian distribution of the light intensity prevented sizes

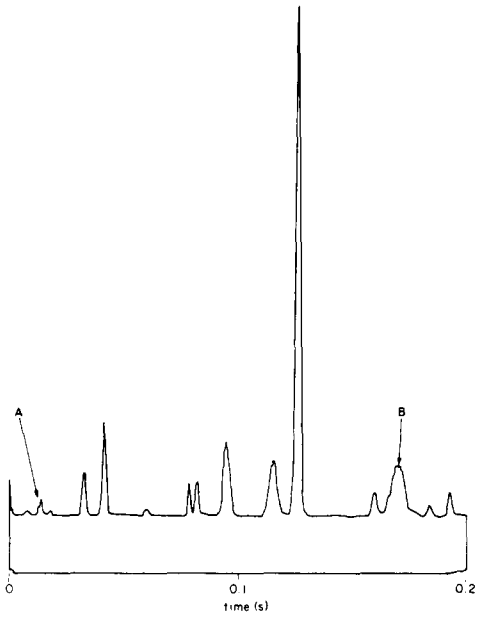

Figure 6 Typical pulse signal at a moderate droplet concentration

from being measured, it did simplify the concentration calculations. The shape of the scattered light signal is the same for a droplet that passes through the middle of the beam as for one that passes through the outer portion so long as they both have the same velocity. The only difference is one of magnitude.[6] All droplets then have the same transient time, which is equal to the beam diameter divided by the droplet velocity. The beam diameter is defined as the diameter with 5 percent of the intensity at the center. The transient time was then 0.00676 s for this study. This theoretical transient time agreed well with the length of the signals recorded on the oscilloscope. Data were collected by randomly starting a trace on the oscilloscope, and the total length of each trace was 0.2048 s. The trace was stored and then recorded and a new trace was made. This process was repeated numerous times for each set of environmental conditions, and the data were later reduced by hand. First the traces were inspected for the possibility of coincident droplets in the measuring volume. These could be readily detected by the shape of the trace as shown at locations A and B in Figure 6. Coincident particles were a problem only at the higher concentrations. Once the traces were corrected, the droplet concentrations were calculated from:[6]

$$C_d = \frac{N_p \tau_s}{t_n V} \tag{18}$$

where V is the scattering volume, t_n is the transient time, τ_s is the length of time for an oscilloscope trace, and N_p is the corrected number of signals for the trace. Typically, about 40 traces were collected for each environmental condition. The concentration data reported here are the averages for all the traces for the stated environmental conditions. In all, more than 2,000 traces were collected.

Experimental results

The experimental data are summarized in Figure 7, where the droplet concentration is shown as a function of air dew-point temperature. Data are grouped according to free-stream air temperature. The line through each data set is simply the least squares line for the data, and no particular physical significance should be given to the line other than to note how rapidly the concentration increases once the dew-point temperature becomes large enough for nucleation to take place. The lines for data sets 1 and 2 terminate at a dew-point temperature equal to air temperature, which is the upper limit for dew-point temperature for the air supply in the test apparatus. The lines for data sets 3–7 terminate at a droplet concentration of 40,000 droplets/cm^3, which was a practical upper limit for droplet concentration measurements. Higher concentrations were difficult to measure because of the problem of coincident droplets in the sample volume. Thus the data for each free-stream temperature were collected up to the maximum dew-point temperature possible in each case. The minimum dew-point temperature for each free-stream temperature was selected to give a maximum saturation in the boundary layer near unity, the condition for which the concentration should drop to zero.

The rapid increase in concentration with an increase in dew-point temperature shown in Figure 7 is to be expected. As dew-point temperature increases, so does supersaturation in the boundary layer, and the critical particle radius for nucleation decreases correspondingly. Because the particle concentration is expected to increase exponentially with a decrease in particle radius, the number of suitable nucleation sites increases rapidly.

The data in Figure 7 can be viewed differently by showing droplet concentration as a function of the theoretical maximum saturation that would occur in the boundary layer without nucleation. The data are presented in this form in Figure 8 and show that only a very small amount of supersaturation is required to produce the heterogeneous nucleation phenomenon. Also, the nucleation phenomenon does not cease at $S = 1.0$ as would be expected, and we do not yet know what causes this result. Only small errors in either the dew-point temperature or the air temperature can cause a significant error in the saturation calculation. The accuracy of using a 1-D boundary-layer equation may also contribute to inaccuracy in the saturation calculation. Finally, turbulent eddies could cause intermittent local supersaturation even though the average local saturation is not greater than unity. Evidence of this action was seen during experimentation.

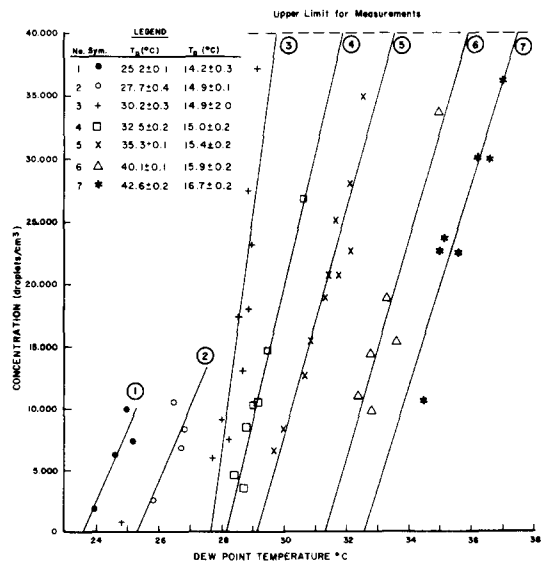

Figure 7 Summary of experimental data

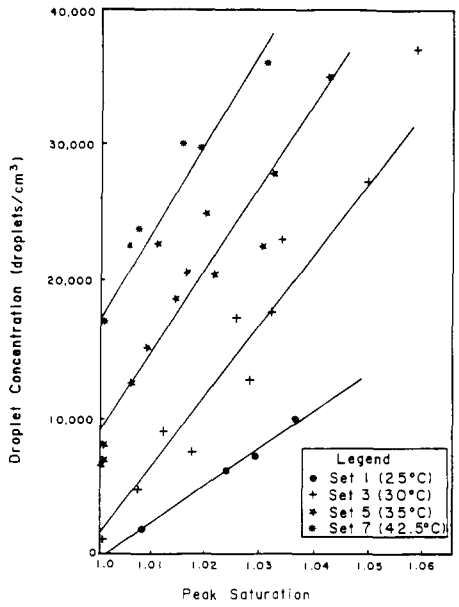

Figure 8 Effect of supersaturation on droplet concentration

Comparison of theory to experimental data

The theoretical calculations require that particle size and concentration distribution be known. In the absence of detailed knowledge of this distribution, the theory of a self-preserving size distribution, as described previously, was used. However, it is still necessary to evaluate C_o in Equation 11. Experimental measurements would be the most desirable way to evaluate C_o, but the necessary instrumentation was not available, and such measurements are not likely to be possible in most practical applications. The approach used in this study was to adjust C_o to obtain the best fit between theory and experiment for one set of data (set 3 in Figure 7) and use this value for all theoretical calculations. The resulting value of C_o was 6.0. This value is not intended for use in other situations but is taken to be representative of the experimental apparatus in this study.

Figure 9 gives a point-by-point comparison of theoretical calculations with the experimental data. For clarity, only four sets of data are included: the lowest air temperature, the highest air temperature, and intermediate air temperatures. As shown, the theory correctly predicts overall behavior but tends to be high at the lower air temperature and low at the higher air temperature.

The theoretical predictions can be represented more concisely by a variable referred to as the nucleation moisture (ϕ). This variable is defined by:

$$\phi = (S_{max} - 1)\frac{\delta_n}{\delta_D} \tag{19}$$

where S_{max} is the maximum saturation that would occur in the boundary layer with no nucleation, δ_n is the width of the nucleation zone, and δ_D is the diffusion boundary-layer thickness. Concentrations of droplets as a function of this variable are shown for both the experimental data and theoretical calculations in Figure 10. It shows, in general, that the theoretical calculations tend to give lower concentrations than the experimental measurements at low values of ϕ and vice versa at higher values of ϕ. The relative magnitudes of the theoretical concentration can be altered by adjusting C_o in Equation 11. However, the shape of the curve does not change so long as the particle-size distribution is assumed to be given by Equation 11. If a different size distribution were used, the model could be altered to give a less rapid or more rapid rise in concentration with increase in ϕ.

Figure 10 also shows that the theoretical predictions are not as sensitive to air-stream temperature as are the experimental data. Again, the difference may be caused by different particle concentrations at the different temperatures. However, there is no particular reason to believe that air temperature will have a major effect on particle concentration in the experimental apparatus. The fact that there is significant nucleation at $\phi = 0$, with the higher air temperatures, indicates that the heat and mass transfer without nucleation may need to be described more completely.

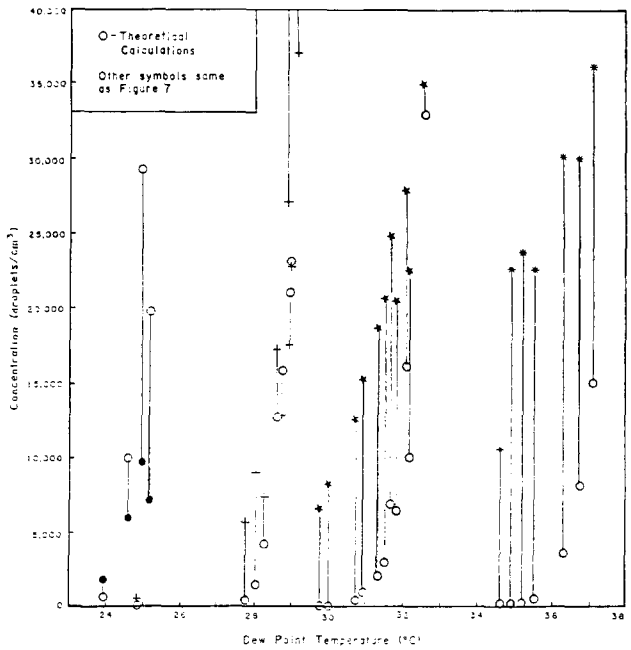

Figure 9 Point-by-point comparison of theory and experiment

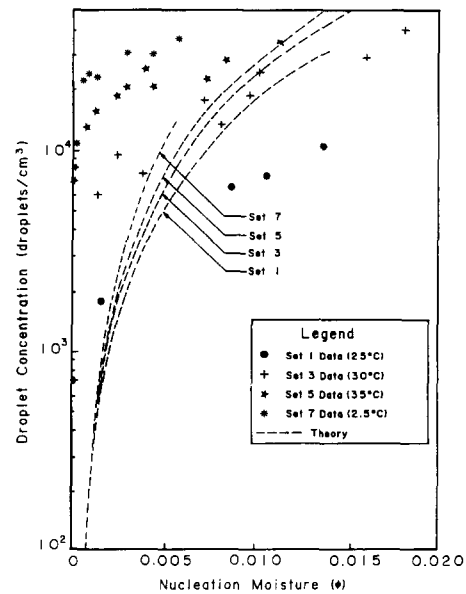

Figure 10 Normalized comparison of theory and experiment

Conclusions and discussion

This study shows that heterogeneous nucleation is a phenomenon that can readily occur under the appropriate conditions in a thermal boundary layer. It also shows that accurately predicting the nucleation rate for a given situation is likely to be difficult. There are several reasons for this inaccuracy. First, the rate of nucleation on particles is very sensitive to local environmental conditions. A small change in either temperature or water-vapor density can result in an order of magnitude change in the nucleation rate for a given size of particle. Second, the number density of particles typically increases inversely with the fourth power of the particle radius. The smallest size of particle that can serve as a nucleation site depends on the local environmental conditions. A very small change in these conditions may result in a small change in the size of particle that can serve as a nucleation site. However, this small change in size can greatly increase (or decrease) the total number of particles that can serve as a nucleation site. Third, the number of droplets nucleated depends directly on the concentration and size distribution of the particles in the air. This distribution is seldom known for most practical applications and usually not even for experimental measurements. For these reasons, it appears that prediction of nucleation is likely to be only an order-of-magnitude calculation in most applications. It should be possible, however, to predict with good accuracy when nucleation can occur.

This study showed that heterogeneous nucleation to some degree can be expected whenever conditions are such that a supersaturated condition arises in the boundary layer. The minimum size of particle nucleated generally is on the order 0.1 μm or less, according to the theoretical calculations. Only filtered air would be free of dust particles of this size. Thus similar heterogeneous nucleation can be expected to occur in almost all situations in which supersaturation arises. This study also showed, at least according to theory, that nucleation mass transport for the situation studied is generally small compared to diffusion mass transport. For the conditions studied, nucleation mass transport ranged from less than 1 percent to a maximum of 10 percent of total mass transport. Thus nucleation considerations are most likely to be of more interest for practical applications where the existence of droplets in the air stream is important. It is unlikely that nucleation considerations can greatly increase the accuracy of total mass transport predictions, at least for the conditions of this study. We recommend that—if the only question that needs to be addressed in a particular situation is whether heterogeneous nucleation takes place—nucleation can be determined by traditional boundary layer calculations that show whether or not supersaturation exists. If it is necessary to determine how changes in conditions will affect nucleation, the calculations presented in this paper are necessary.

We recommend that future research be conducted in two areas: (1) theoretical equations and solutions should be developed for a 2-D description of the boundary layer; and (2) experimental measurements should be conducted with particle concentration, particle composition, and size distribution accurately measured in the range of 0.01 μm to 1.0 μm.

References

1 Byers, H. R. *Elements of Cloud Physics*. The University of Chicago Press, Chicago, 1965

2 Mason, B. J. *The Physics of Clouds*, 2nd ed. Clarendon Press, Oxford, 1971

3 Volmer, M. *Kinetik der Phasenbildung*. Steinkopff, Dresden and Leipzig, 1939

4 Bird, R. B., Stewart, W. E., and Lightfood, E. N. *Transport Phenomena*. John Wiley & Sons, New York, 1960

5 Epstein, M. Nonequilibrium fog formation within the thermal boundary layer. Ph.D. dissertation. Polytechnic Institute of Brooklyn, NY, 1969

6 Chen, M. S. The condensation by heterogeneous droplet nucleation in boundary layers. Ph.D. dissertation, Kansas State University, Manhattan, KS, 1984

7 Davis, B. L. *Nucleation Processes in Cloud Physics*. South Dakota School of Mines and Technology, Rapid City, SD, 1976

8 Fletcher, N. H. Size effect in heterogeneous nucleation. *J. Chem. Phys.*, 1958, **29**, 3

9 Rogers, R. R. and Yau, M. K. *A Short Course in Cloud Physics*, 3rd ed. Pergamon, New York, 1989

10 Clark, W. E. and Whitby, K. T. Concentration and size distribution measurements of atmospheric aerosols and a test of the theory of self-preserving size distribution. *J. Chem. Phys.*, 1967, **24**

11 Allen, T. *Particle Size Measurement*, 3rd ed., Powder Technology Series. Chapman and Hall, New York, 1976